ELSEVIER

Thin Solid Films 311 (1997) 1–6

thin solid films

Corrosion of sputtered W–Ni–N hard coatings in chloride media

Christopher M.A. Brett *, Crina-Maria Nimigean

Departamento de Química, Universidade de Coimbra; P-3049 Coimbra, Portugal

Received 21 April 1997; accepted 13 May 1997

Abstract

The corrosion behaviour of sputtered W–Ni–N hard coatings of 4 μm and 8 μm thickness on high speed steel substrates and with different percentages of nitrogen has been evaluated by electrochemical techniques in aqueous chloride solution and by scanning electron microscopy. It was found that the incorporation of nitrogen in the films increases the corrosion resistance. Corrosion occurs mainly by pitting through to the substrate; in comparison to similar W–Ti–N coatings, the corrosion rate is greater. © 1997 Elsevier Science S.A.

Keywords: Thin films; Hard coatings; Sputtering; Corrosion; Pitting; Tungsten–nickel

1. Introduction

The modification of the surface of high speed steel by thin film sputtered hard coatings, thickness 1–10 μm, based on W–C with other incorporated elements such as Co in order to increase the wear resistance has been the subject of a number of publications in recent years, e.g., [1–3]; encouraging results have also been obtained with W–N films [4]. The films obtained tend to be compact and homogeneous with low porosity. For use in real situations such as cutting tools, a good corrosion resistance is also important; however, not much work has been done on the electrochemical behaviour of sputtered thin films. Nevertheless, it was found that the substitution of Co by Ni in the W–C–Co cemented carbide system gave rise to increased corrosion resistance [5], suggesting the potential importance of films incorporating nickel.

Recent work concerned the characterisation of the electrochemical behaviour of thin films of W–Ti–N coatings on M2 high speed steel [6]. The main conclusion of this work, carried out by various voltammetric techniques, impedance spectroscopy and scanning electron microscopy, was that corrosion occurs preferentially at microscopic sites in the sputtered films and that increased film thickness can reduce the probability of its occurrence. From this it was deduced that flaws in, or underneath, the as-deposited coating could be responsible. An increase of the nitrogen content of the films also reduced the corrosion rate, but to a lesser extent.

In this work, a similar type of study has been undertaken for films of the type W–Ni–N. The high temperature oxidation of these films has been investigated and they show a higher oxidation resistance than W–Ti–N films [7]. Four film compositions were studied, varying from each other in film thickness and nitrogen content.

2. Experimental

The substrates were heat-treated cylinders, diameter 12 mm and thickness 3 mm, of M2 steel (W 6.4; Mo 5.0; Cr 4.2; V 1.9; C 0.86; Si $<$ 0.4; Mn $<$ 0.4%). After polishing to a mirror finish with diamond paste they were sputter-coated on one face in a Hartec dc magnetron sputtering apparatus. Before deposition, the surface was degreased and the cleaning procedure included heating and argon ion etching under vacuum. Deposition was done from a W + 10 wt.% Ni target at a power density of 11 W cm^{-2} and a negative substrate bias of 70 V. The total gas pressure employed was 0.3 Pa; the gas was a mixture of nitrogen and argon, the ratio of N_2/Ar partial pressures was varied in the range $0-\frac{1}{3}$. Each sputtering deposition led to ten samples with uniform coating thickness. The four types of sample produced for electrochemical experiments are shown in Table 1.

The coated samples were transformed into electrodes by attaching a copper wire to the rear face with silver epoxy

* Corresponding author. Tel.: +351 39 35295; fax: +351 39 35295; e-mail: brett@cygnus.ci.uc.pt

0040-6090/97/$17.00 © 1997 Elsevier Science S.A. All rights reserved.

Table 1
Characteristics of the sputtered W–Ni–N films

Film type	Film composition (wt.%)	N_2 partial pressure (Pa)	Film thickness (μm)
1	W (97.3), Ni (2.7)		4.0
2	W (97.3), Ni (2.7)		8.0
3	W (76.2), Ni (12.7), N(11.1)	0.06	4.0
4	W (66.5), Ni (12.1), N (21.4)	0.11	4.0

and protecting the whole assembly, except for the coated face, with epoxy resin and varnish. The electrochemical cell also contained a platinum foil counter electrode and a saturated calomel electrode as reference. All experiments to be described were carried out using a solution of 0.1 M potassium chloride prepared from analytical grade reagent and ultrapure water (Millipore Milli-Q, resistivity > 18 MΩ cm). Solutions were not deaerated.

Corrosion potential measurements were done with a Schlumberger S17151 Computing Multimeter and voltammetric experiments with a PC-controlled EG&G PAR273A potentiostat using PAR Model 352 software. Impedance measurements were carried out using a Solartron 1250 Frequency Response Analyser coupled to a Solartron 1286 Electrochemical Interface using a 5 mV rms perturbation in the frequency range 65 kHz to 10 mHz and controlled by ZPlot software; simulations were performed with ZSim CNLS software.

Scanning electron microscopy was done with a Jeol T330 Scanning Electron Microscope equipped with a Tracor Northern Microanalysis Accessory.

3. Results and discussion

3.1. Corrosion potential

The variation of corrosion potential with time during the first hour of immersion is shown in Fig. 1 for all samples. In contrast to the substrate [8] and to films of W–Ti–N [5], after the initial sharp variation of potential in a negative direction there is some variation towards positive potentials, Fig. 1b, before a further movement in the negative direction. This indicates that pits have been formed and the elapsed time can be associated with the pitting induction time. There is convergence of the values after several hours except for Type 4 films, i.e., those with the larger percentage of nitrogen, which are undergoing a lower rate of corrosion. So nitrogen appears to have a beneficial effect.

The plots in Fig. 1 show significant differences relative to the W–Ti–N films in Ref. [6] where no such oscillation in corrosion potential was found. This different type of profile must therefore be due to the presence of nickel in the film and suggests the occurrence of passivation through the formation of nickel hydroxide species. Corrosion potential values tend towards those expected for M2 steel at long immersion times in 0.1 M KCl of -0.60 V vs. SCE [8]. Thus, the corrosion potential reflects the corrosion resistance of the film itself initially and, at longer times, reflects principally the corrosion of the substrate where film breakdown has occurred—this is visible to the naked eye, see below.

In order to test the hypothesis that corrosion occurs mainly at specific microscopic sites in the as-deposited coatings, samples were corroded for 1 h in potassium chloride solution and then removed, washed with distilled water and dried. The surface was examined with a low-magnification microscope and points where corrosion was observed to be commencing were covered with tiny quantities of epoxy resin to insulate them from the solution. These corrosion sites appeared in a completely random

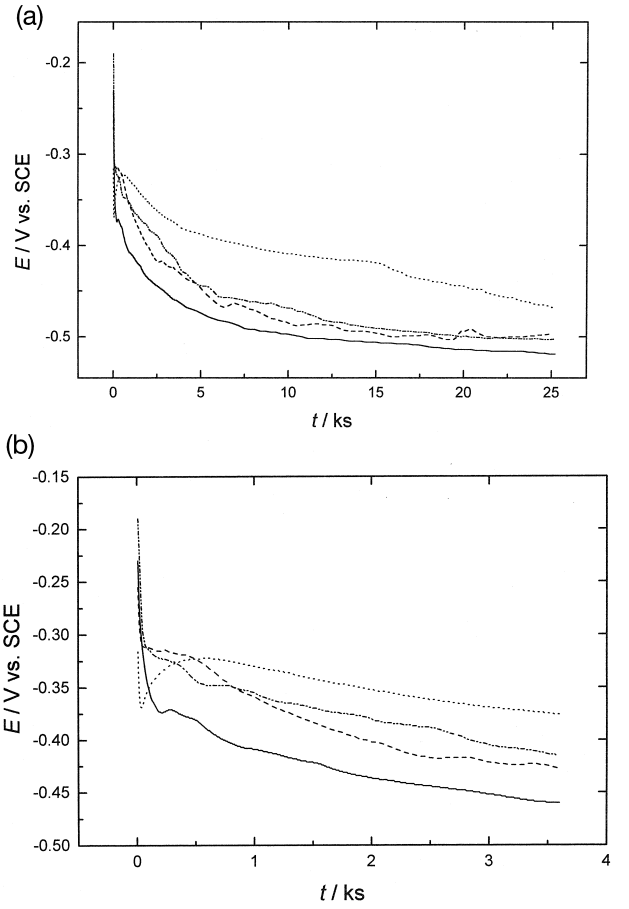

Fig. 1. (a) Plot of E_{cor} vs. t for samples coated with films Types 1–4: (————) Type 1; (——) Type 2; (-·-·-·-·-) Type 3; (·····) Type 4. (b) Enlargement of (a) during the first hour of immersion.

Table 2
Results from polarization resistance measurements, R_p

Film type	R_p (kΩ cm^2)	
	$t = 5$ min	$t = 1$ h
1	9.9	6.8
2	5.7	8.2
3	6.7	8.4
4	20.2	8.0

way over the surface of the film; typically, eight to ten sites appeared over the area of ~ 1.0 cm^2. When the glue had dried the sample was re-immersed; the corrosion potential after re-immersion was more positive than just before removal. As an example, a W–Ni film sample had $E_{cor} = -0.45$ V just before removal from solution after 1 h immersion; 10 min (to allow stabilisation) after reimmersion, following insulation of the corrosion sites, the value was -0.38 V vs. SCE; such changes in a positive direction of between 0.05–0.07 V were found in all cases. Corrosion, as manifested through the negative variation of corrosion potential, continued but was less and without periodic oscillations. The emergence of new localised points of corrosion was not observed.

3.2. Polarization resistance

From the above, it is clear that important information relating to the corrosion resistance of the film without the influence of microscopic corrosion sites is best obtained in experiments conducted shortly after immersion. Linear polarization resistance experiments, commenced 5 min after immersion, and done within ± 20 mV of the corrosion potential at a scan rate of 0.1 mV s^{-1}, are therefore appropriate for this purpose. Polarization resistance values, R_p, determined in this way are collected in Table 2 and suggest strongly that an increase in film thickness has no beneficial effect, whereas an increase in nitrogen content does, contrary to what was found for films of the type W–Ti–N [6]. This is also in agreement with the corrosion potential results in Section 3.1.

Additionally, Table 2 gives R_p values after 1 h immersion—particular care was taken in not agitating the solution during this time. The values are now similar for all coatings, suggesting that where corrosion has occurred direct access of the solution to the corroding sites on the surface becomes more difficult, probably due to blocking by a coating of hydroxy-type corrosion products. This is not necessarily inconsistent with the E_{cor} values in Fig. 1, since R_p represents the value of dE/dI close to the corrosion potential.

3.3. Potentiodynamic behaviour

Plots of E vs. log I were recorded for all types of sample in order to determine Tafel parameters. These are

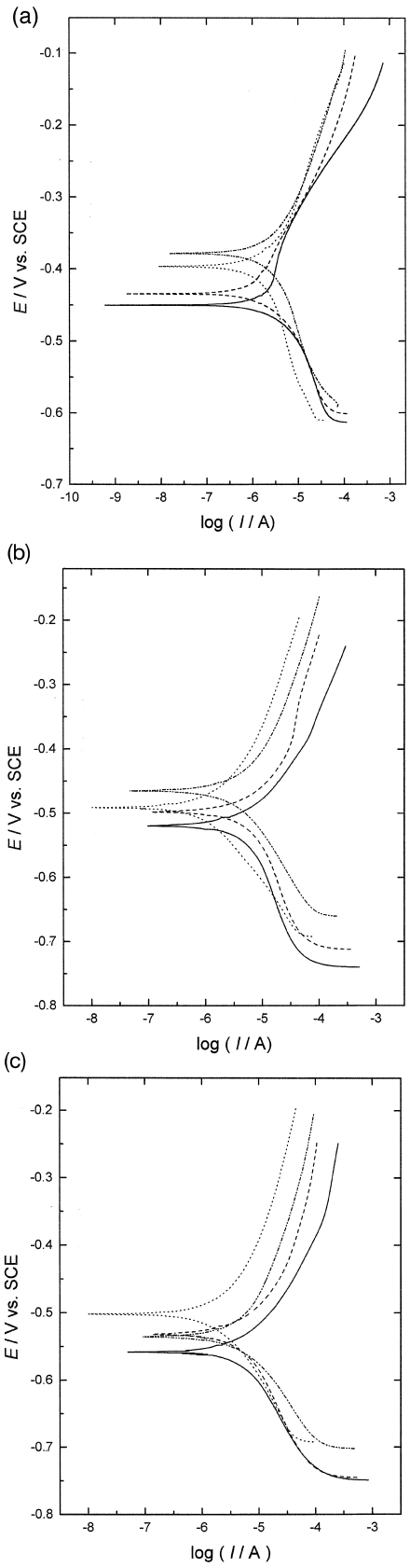

Fig. 2. Tafel plots for all samples after immersion times of (a) 10 min, (b) 1 h, (c) 4 h: (————) Type 1; (——) Type 2; (-·-·-·-·-) Type 3; (·····) Type 4. Scan rate 2.5 mV s^{-1}.

shown in Fig. 2 for three different immersion times—10 min, 1 h and 4 h. They show clearly that Type 1 films undergo greatest corrosion and that increasing nitrogen content as well as increasing film thickness are beneficial. Although Type 3 films appear to be better than Type 4 films at short immersion times, the order is already reversed after 4 h immersion.

Fitting of the curves obtained using ParCalc (included in M352 software) leads to the corrosion currents and corrosion potentials shown in Table 3. Values of corrosion potential are consistent with those in Fig. l within experimental error. Corrosion currents are low and diminish with increasing nitrogen content. Also, there is an unexpected increase with increasing film thickness after 1 h or more immersion. It is tempting to attribute this to a defective sample but repetition gives similar results. Additionally, electrochemical impedance experiments give similar information, see below.

Table 3
Tafel plot analysis

Film type	I_{cor} (μA cm-2)			$-E_{cor}$ (V vs. SCE)		
	10 min	1 h	4 h	10 min	1 h	4 h
1	1.8	9.9	8.7	0.45	0.52	0.55
2	2.5	13.2	22.2	0.43	0.50	0.53
3	5.3	6.5	7.6	0.38	0.47	0.53
4	2.7	1.9	3.6	0.40	0.49	0.50

3.4. Electrochemical impedance

Typical impedance spectra for Type 3 films are given in Fig. 3. These show a semicircle corresponding to a charge

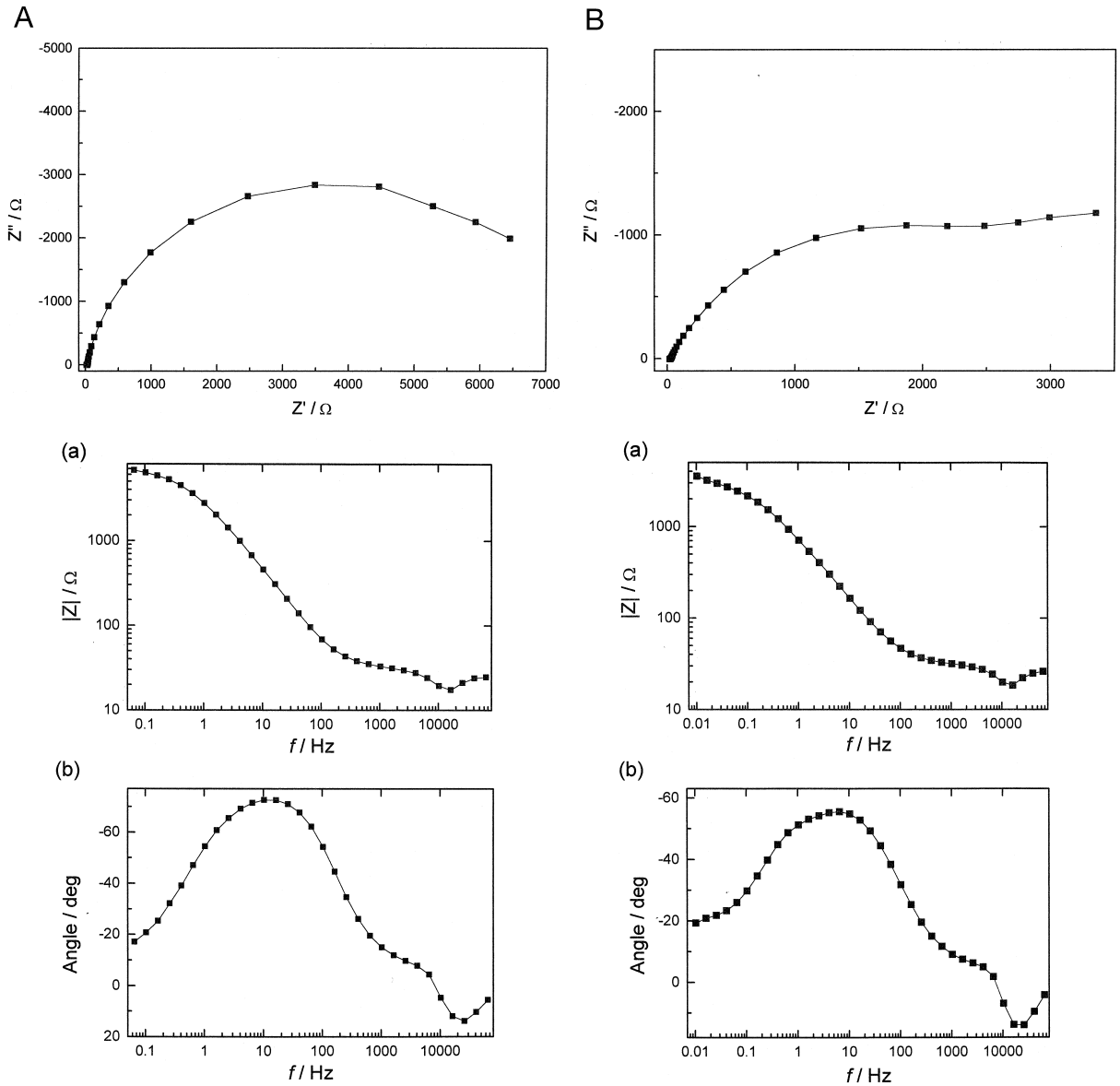

Fig. 3. Complex plane and Bode plots for the electrochemical impedance of Type 3 film at a potential equal to E_{cor} after immersion during (a) 10 min and (b) 1 h.

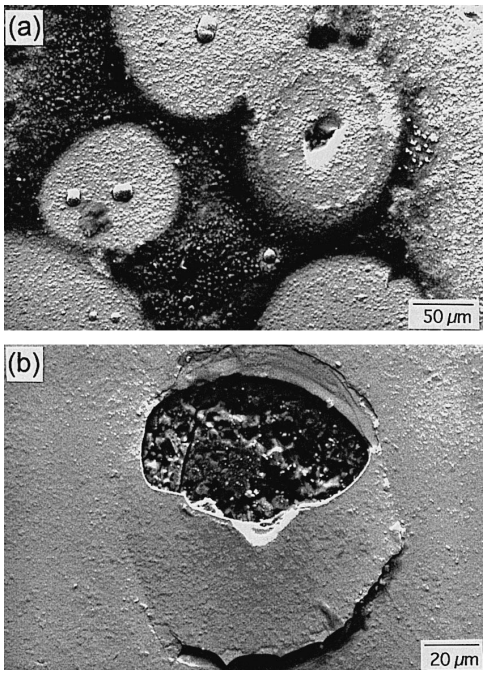

Fig. 4. Features from scanning electron microscopy of the coating surfaces: (a) Type 2 film (b) Type 4 film.

transfer process and indications of a finite Warburg impedance at low frequency; the absolute impedance values diminish with increasing time. The diameter of the semicircle is a direct measurement of the charge transfer resistance. These values were obtained by CNLS fitting of the data at frequencies above 1 Hz to an equivalent electrical circuit, taking into account the rough nature of the interface. Besides the solution resistance contribution, this is composed of an *RC* parallel combination (this *R* is identified in the analysis with R_{ct}, the charge transfer resistance) modified by a constant phase element in series with another resistance, see Fig. 4. Table 4 shows that in all cases there is a reduction in R_{ct} with time, although the largest decrease is that shown by Type 4 films, the W–Ni–N film with largest percentage of nitrogen.

Table 4 shows that, after 1 h immersion, that Type 2 samples, W–Ni 8 μm, have the largest rate of corrosion. This is similar to the observed behaviour through recording of Tafel plots, see Table 3 and previous section. Such surprising behaviour leads one to speculate on changes in film structure as its thickness is increased, and will be discussed after presentation of the morphological observations.

Table 4
Values of charge transfer resistance, R_{ct}, from impedance plots

Film type	R_{ct} (kΩ cm^2)	
	$t = 10$ min	$t = 1$ h
1	2.56	2.50
2	4.00	1.92
3	5.60	2.40
4	5.60	2.80

3.5. Morphological observations

Scanning electron microscopy confirmed, as for W–Ti–N [6] and as suggested by the electrochemical results, that corrosion is occurring in localised areas. In the two micrographs shown in Fig. 4 one can distinguish zones which have not been attacked, zones where corrosion is commencing and zones where corrosion has already occurred and where the substrate has been corroded.

Chemical microanalysis of sites where the substrate has already been attacked as in Fig. 4a shows that the detritus around the pit (at a distance approaching 50 μm in this case) is predomi-nantly iron oxides and that the elemental composition within the pits has a higher predominance of the elements other than iron than that measured for the uncorroded M2 steel substrate. This was also found in a study of the corrosion of the M2 steel substrate [8] and suggests that the iron phase is undergoing corrosion leaving the carbide particles (dimension ≤ 4 μm) largely untouched.

Also shown in Fig. 4a are sites with the morphology of a (almost hemispherical) bubble with the chemical composition of the film, at the centre of the area where corrosion appears to be occurring, as shown by the deposited iron oxide. In this context, Fig. 4b is of particular interest, which shows a conformation similar to a burst bubble, and indicates diffusion of the attacking species through the coating. A number of these features were found on the samples and this probably represents the physical mechanism of coating corrosion. These aspects are currently being investigated further in order to propose a more detailed model of coating corrosion in these media.

3.6. Final remarks

Electrochemical techniques employed in this study show the beneficial effect on increasing corrosion resistance of the addition of nitrogen to W–Ni films, the greater the percentage nitrogen the larger the resistance. This can be attributed principally to the amorphous nature of the W–Ni–N films [7]. It has also been shown that care must be taken to produce flawless coatings in order to avoid sites where corrosion can more easily commence. The mechanism of corrosion appears to involve the formation of bubbles in the film which then burst revealing a pit in the substrate.

It is also important to discuss the surprising result from Tafel plot analysis and electrochemical impedance that for immersion periods of the order of 1 h and longer, the corrosion rate is higher for the 8 μm W–Ti films than for the 4 μm films. In fact, it is known that on increasing the thickness of sputtered films, the cross-section morphology

becomes less compact near the surface [9], thus permitting penetration of electrolyte to within the film. In this way the conditions for commencement of pitting corrosion could be more easily created. Such a process would be slow, explaining the period of 1 h necessary for the consequences to become microscopically observable.

4. Conclusions

This study has shown the importance of nitrogen content in increasing the corrosion resistance of films based on W–Ni–N on high speed steel substrates, which may be due to changed film characteristics. Electrochemical behaviour within the first few minutes after immersion in electrolyte solution reflects the characteristics of the coating as a whole, whereas changes at longer times are probably due to corrosion commencing at microscopic corrosion sites, possibly flaws, in the film.

Acknowledgements

Financial support from Junta Nacional de Investigação Científica e Tecnológica (JNICT), Portugal, project PBIC/C/CTM/1383/92, and from Tempus programme JEP-04223-95/3 is gratefully acknowledged. We thank Dr. A. Cavaleiro for discussions and for the scanning electron microscopy.

References

[1] A. Cavaleiro, M.T. Vieira, G. Lemperière, Thin Solid Films 197 (1991) 237.
[2] A. Cavaleiro, M.T. Vieira, G. Lemperière, Thin Solid Films 213 (1992) 6.
[3] A. Ramalho, S. Fayeulle, M.T. Vieira, Thin Solid Films 254 (1995) 131.
[4] W.J. Tomlinson, C.R. Linzell, J. Mater. Sci. 23 (1988) 914–918.
[5] C. Ringas, F.P.A. Robinson, S.B. Luyckx, J.P.F. Sellschop, Surf. Eng. 6 (1990) 194.
[6] C.M.A. Brett, A. Cavaleiro, Mater. Sci. Forum 192–194 (1995) 797.
[7] C. Louro, A. Cavaleiro, Surf. Coat. Technol. 74–75 (1995) 998.
[8] C.M.A. Brett, P.I.C. Melo, J. Appl. Electrochem. 27 (1997) 959.
[9] R. Messier, A.P. Giri, R.A. Roy, J. Vac. Sci. Technol. A 2 (1984) 500.